Some Physics Considerations of Magnetic Inertial Electrostatic Confinement: A New Concept for Spherical Converging Flow Fusion

By Robert W. Bussard, Energy/Matter Conversion Corporation, 680 Garcia Street, Santa Fe, NM 87505, (505) 988-8948, <emc2qed@comcast.net>

Abstract

A new concept for inertial-electrostatic spherical colliding beam fusion (Polywell) is based on the use of magneto-hydro-dynamically stable quasispherical polyhedral magnetic fields to contain energetic electrons that are injected to form a negative potential well that is capable of ion confinement. A simple phenomenological model for this system shows that:

1. It is grossly stable against internal and global perturbations by virtue of the effects of both the external magnetic fields (typically 1 to 5 kG) and the large central azimuthally isotropic power flow due to conservation of transverse momentum in the recirculating ion flow.
2. Electron current recirculation ratios must be of the order of 10^5 for net fusion power operation, which is found to be possible within limits set by energy-exchange self-collisions.
3. Losses due to bremsstrahlung and synchrotron radiation can be kept small relative to fusion power generation, and ion energy Maxwellianization by two-body collisional up-scattering can be kept to acceptable levels by operation at sufficiently large well depth.
4. System gains of 10 to 100 seem possible from several fusion fuels.
5. No zero-order impediments have yet been found to this highly speculative concept; feasibility must be determined by study of more complex and detailed phenomena.

I. Introduction and Background

I.A. The Basic Concept

A new method of energizing and confining charged particles has been devised[1] that offers promise for efficient small-scale control of their motion in spherically converging recirculating flow and for the generation of fusion reactions among them. This method uses special magneto-hydro-dynamically (MHD) stable magnetic field configurations to confine energetic electrons that are injected to form a negative potential well that is within the volume bounded by the magnetic fields. These fields consist of point cusps arranged in an alternating pattern in a generally spherical geometry around the confinement region, such that they occupy the faces of polyhedra with an even number of faces around each vertex.

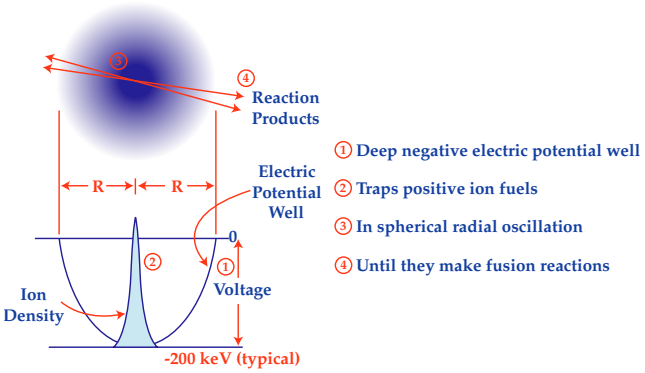

Figure 1 — Inertial-electrostatic confinement

Energetic positive ions may be confined by the negative potential well formed by injection of energetic electrons into the magnetic field system. Ions supplied to the system gain energy by falling into this well. Ion and electron currents build up to large values limited principally

by electron losses through cusps and by the loss of ions in charged-particle fusion reactions that release energy and create highly energetic fusion product particles that escape from the confined volume. The basic principles of operation of this concept for confinement, called the Polywell, are shown in Figures 1 and 2. The principal physics phenomena of importance fall logically into five main classes:

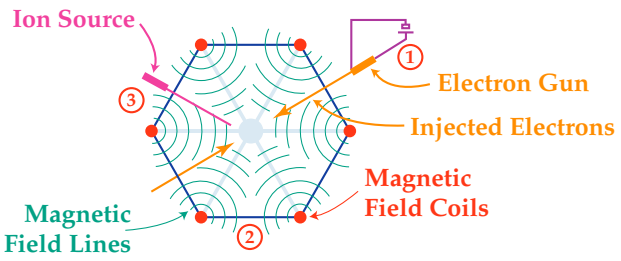

① Trapping well formed by energetic electron injection

② Cusps of polyhedral magnetic field

③ Ions fall into well and remain until reacted

Figure 2 — Inertial-electrostatic confinement

1. Phenomena of electron injection at high energy to form a negative well with a strong virtual cathode and of electron losses and stability, directly through the field structure and as affected by the polyhedral magnetic fields
2. Effects of positive ion injection at low energy into such wells, ion confinement, loss phenomena, and distribution and energy as influenced by magnetic fields, and by electron injection energy and net injection current
3. Dynamic phenomena associated with spherical electrostatic waves and conditions for their onset and growth: effects on confinement, well depth, potential distribution, and stability as influenced by net ion current, and field and electron conditions
4. Collisional effects on ion and electron energy distribution, particle confinement, and loss rates for scattering and energy-generating collisions between various charged-particle species and the effects on stability of charged-particle interactions
5. Concept/device potential and parametric limits, definition of physics and engineering features and constraints, and engineering performance characteristics of candidate applications systems.

The potential performance of this concept is determined by the interaction of physical processes in each of these five areas. More detailed examination of these phenomena is given here and in a recent study[2] of the concept.

I.B. Prior Work

Most fusion research since 1952 has been based on magnetic confinement of Maxwellian plasmas, but the use of electric fields for confining ions was also noted as an approach worthy of study. Physics studies applicable to electric confinement originated with work by Langmuir et al.[3] in the early 1920s, who analyzed current distributions as limited by space charge in planar, cylindrical, and spherical geometries. These studies formed the basis for developments in high-power gas tubes in the 1940s and 1950s, and for ion magnetron tubes and toroidal dense electron confinement devices of the 1960s.[4] Concepts for electric confinement were discussed by Lavrent'ev[5] and research programs were conducted in the USSR and France,[6] without notable success.

Work in the United States has been limited to a few small efforts in university and government laboratories, and to one significant effort under private industrial auspices by Farnsworth[7] and Hirsch,[8] who pioneered inertial-electrostatic concepts for confinement. Their limited research yielded encouraging results. When their work essentially stopped in the late 1960s, laboratory experiments had shown fusion neutron production at rates of ~10^{10} neutrons/second — still a world record for steady-state output.

Analytical and numerical simulation studies were made of these latter systems by Hu and Klevans,[9] Black,[10] Barnes,[11] and others, which showed the effects of transverse momentum in the spherically converging flow systems and illustrated problems of ion convergence and virtual electrode formation associated with these and with considerations of collisional effects.

Initial research concepts came from the field of gaseous electronics, and early electrostatic studies made little use of externally generated magnetic fields. In contrast, studies in the field of fusion research focused almost entirely on attempts to confine plasmas with magnetic fields. Purely electrostatic confinement concepts studied in the past[12,13] were thought to have limitations that prevented achievement of the high particle densities and stable confining field configurations needed for large reaction rates. These difficulties included:

a. Potential well instability under displacement of confined particles.
b. Excessive particle leakage from electrostatic grid-driven confinement volume.
c. Particle collisional and energy losses to walls and to electric grid structures that provided the confining potential well configuration.

II. Summary of Technical Features and Characteristics

The concept considered in this paper overcomes the foregoing difficulties by use of external magnetic field confinement of radially injected energetic electrons that create an ion-confining electric potential well. The confined quasi-spherical volume is formed from a special polyhedral array of magnetic surface point cusps, yielding internal field strength $B(r)$ decreasing toward the center. The collisional loss rates from such point-cusp systems are two to three orders of magnitude less than those through the line or equatorial cusp geometries utilized in traditional magnetic mirror confinement geometries.[14] These "surface" fields provide a steady-state, quasi-spherical surface confining effect capable of maintaining higher electron density within the system than is otherwise possible. The confined electrons establish a kinetically driven electrostatic negative potential well whose field strength $E(r)$ and well depth E_{-w} are determined by their injection energy and transverse momentum, the efficacy of their confinement by the magnetic field, and by the balance between total injected ion and electron currents. This negative well attracts positive ions injected at low energy or allowed to "fall" into the well and imparts energy to these equal to their fall through the negative well, acquiring radial velocity $-v_i(r)$ as they move into the system. For example, if E_{-w} = 100 keV deep, all of the ions falling into the system will arrive at the bottom of the well (at the system center) with 100-keV energy.

The motion of the ions can be made to be nearly purely radial in most of the well (where $-v_i \times B/c << E$) so that ion density varies at least as rapidly as the inverse square of the radial position $n_{-i} > 1/r^2$. The resulting variation of collision density for reactions of any type (scattering, energy generation) is as the inverse fourth power (or higher) of radius $1/r^4$. Nearly all collisions occur very close to the system center, ensuring that they will only redirect the momentum vector of the particles along differing radial lines and will not lead — at least to zero order — to the direct collision-driven spatial losses found in all conventional magnetic confinement systems.

This is a natural result of the spherical geometry of ion motion so that two-body collisions always occur with equal momentum at or near the system center of geometry (CG) for particles with equal mass [e.g., deuterium-deuterium (D-D), ^{3}He^{3}He, ^{6}Li^{6}Li, tritium-tritium, T^{3}He]. The case of particles of differing mass is more complex, but the same result is found if these are introduced into the potential well with total energies in inverse proportion to their masses [i.e., with equal momenta in the collisional center-of-mass (CM) frame of reference].

Central collisions drive the initial monoenergetic ion energy distribution toward radial Maxwellian, but proper choice of operating conditions can minimize the effects of such broadening. Over the collisional lifetime of a typical ion before it undergoes fusion, the number of two-body collisions can be kept less than is required to cause significant losses from the system. Three-body and many-body collisions always scatter particles and spread (and upscatter) energy distributions, but these are very much less probable (e.g., 10^{-6} of the two-body rate) at densities of interest.

The field geometries are all inherently MHD stable because they are everywhere convex toward the confined region. Unstable cross-field turbulent enhancement of electron surface transport losses is not favored because the electrons are at their highest energy and lowest density in the outer region, electron-electron collisions are least probable, and transverse electric perturbation fields cannot be sustained in the magnetically constrained spherical geometry. Collisional scattering and direct propagation loss of electrons through the field cusps constitute a major loss mechanism for electrons, but this is not a source of instability for ion transport.

The only significant instability identified was pointed out by Elmore *et al.*[12] and later by Furth[13] as that due to a local displacement of plasma electrons or ions from the otherwise spherical spatial distribution that they will assume under the action of the inertial electric forces in the system. A small displacement of this sort [e.g., displacement motion toward a prolate (or higher order) figure] can give rise to a local current and thus to a local B field encircling the displaced volume. This, in turn (as a version of the "pinch" effect), drives further displacement of the volume by the magnetic pressure force ($B^2/8\pi$) around it, deriving from the current. Near the well center, the restoring force due to the potential gradient is small since the E field is identically zero at r = 0, and the displacement is unstable in the absence of other restoring forces.

At the system center, the principal restoring force is not that of the E field but rather that due to the counter-streaming interaction of particles moving through the central region, which couple their momenta to each other through spherical electrostatic waves. Such waves arise from current-density-driven, bounded, multi-stream instabilities that occur naturally as the current density increases strongly toward the center. The stabilizing energy density available from momentum transfer in this radial flow vastly exceeds any possible local perturbation B field energy density that can be generated by local particle displacement. At the system surface, the restoring forces are simply due to the imposed external magnetic field, which prevents any radial perturbation displacement of electrons (or of the ions) and ensures the quasi-sphericity of the gross system. Instabilities

may occur in the countercurrent flows in the midrange of radius $0 < r < R$ that cause the electric field to be distorted by density distribution displacements; effects of these are not addressed in this paper.

Production of fusion reactions occurs predominantly at the device center, where particle densities are highest. The magnetic fields are zero at this point; thus, synchrotron radiation does not constitute an energy loss mechanism from the reacting region. Synchrotron radiation can take place at the cavity boundary, from electrons moving at their highest speeds, but the energy loss rates are found to be small and can be kept very far below those due to electron particle cusp leakage losses. The only remaining significant source of radiation loss is from electron-ion bremsstrahlung collisions taking place in the central region. Study of the scaling of this radiation shows that it can be kept well below the charged-particle reaction power, if the system is made to operate at well depths such that the fusion reaction cross sections are above a few hundredths of a barn (10^{-24} cm^2).

Analysis shows that the power required to drive such devices may be less than their power output capability (if the method works at all) and may allow the development of power amplifiers with high gain.

The mechanisms of well generation, particle confinement, and reaction are all electrically controlled and relatively independent of the type of charged particle used. As a result, it is possible, in principle, to operate in either steady-state or oscillatory input-output modes and to use any combination of ions that produces energy when undergoing nuclear collisional rearrangement reactions. For example, charged-particle reactants may be used whose reaction products are only other charged particles and are free of direct nuclear radiations (i.e., no fast neutrons are produced). Most of these product particles have energies greatly in excess of the confining potential well; thus, they can "climb" out of the well and act against externally imposed field gradients. Direct conversion of particle energy to electricity is evidently possible for such reactions, as suggested in Figure 3, by the use of relatively standard approaches.[15,16,17]

Operation with such reactants could be of use for systems in which energy generation without nuclear radiation is desirable (e.g., for aerospace propulsion applications or for space power generation) or in which oscillatory output may be desired (e.g., as direct reaction-power self-amplification of oscillatory input microwave signals). Alternatively, reactants may be chosen whose principal products are energetic fast neutrons, as may be useful for some types of defensive nuclear systems or for systems in which fissionable fuel breeding is desired or neutron transmutation burn up of fission product wastes is a primary goal.

III. Negative Potential Well Formation by Electron Injection

III.A. Constant Charge Density and Inertial Effects

In a spherical volume of radius R, in which a net uniform charge density is held fixed, Poisson's equation can be solved directly to give the net charge and corresponding particle density required to produce a potential well of arbitrary depth. From its solution, the charge density required is:

$$\delta n^- = \left(\frac{3E_w}{2\pi e R^2}\right) = \delta n^- = 3.32x10^6\left(\frac{E_w}{R^2}\right) \quad (1)$$

where:

e = electronic charge

δn^- = $(n^-) - (n^+)$ = net negative charge density (particle/ cm^3)

E_w = well depth (eV)

R = radius (cm)

Numerical examples (e.g., R = 100 cm, E_w = 10^5 eV, requires δn^- = 3.3 x 10^7/cm^3) show that only a very small net charge density is sufficient to create very large negative potential wells, even with uniform and constant charge density.

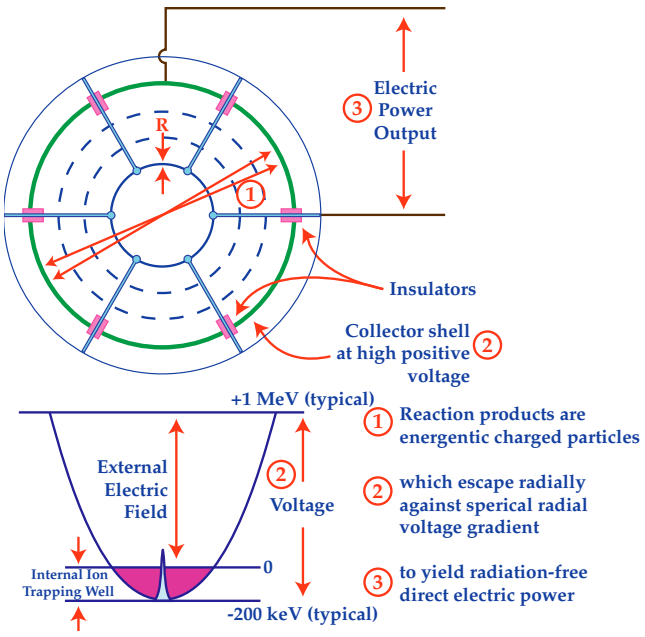

Figure 3 — Direct electric conversion

However, in the actual system of interest, both the positive and negative charges are moving rapidly through the well region at greatly varying speeds and with greatly varying densities.

In such a well, an approximate idea of particle motion can be found by simple analyses using an assumed potential distribution such as a parabolic potential well, given by:

$$E_w(r) = E_w[1 - \langle r \rangle^2] \quad (1b)$$

where $\langle r \rangle = (r/R)$. Using this, the ion and electron densities ($n_{\sim i}$, $n_{\sim e}$) in the system can be related to the electron density $n_{\sim eo}$ and the ion and electron injection energies (E_{io}, E_{eo}) at the surface $r = R$. Electrons are injected with large energy, and ions are allowed to fall into the negative well with small injection energy. Radial electron flow is inhibited toward the center by conservation of transverse (angular) momentum induced by the electron reflection process in the surface field. The convergence of ions is similarly limited, but to a lesser degree, because their induced transverse momentum is (or can be made) much less than that for the electrons and their radial momentum content is much greater. This is because the electrons have maximum speed where B is highest (at $r \approx R$) while ions can be kept away from the high B field region by interior injection, so that ion speed is always small where B is large.

Without ions, an inward flow of radially monoenergetic electrons with finite angular momentum at the surface would stop at that radial position r_f at which their angular kinetic plus electrostatic potential energy equals their initial total kinetic energy. A sharp virtual cathode is formed. Within this radius, the well is flat at depth $E_{\sim w}$. In the real case, the electrons have an energy spread comparable to that induced tangentially in the reflection process, and strong ion currents are flowing through the hypothetical virtual cathode radius, carrying electrons on into the well. The radial motion of electrons outside this critical radius is constrained by conservation of both radial current flow and angular momentum.

To assess this, it is first necessary to estimate the variation of ion and electron densities and speeds with radial position in the potential well. This is a complex problem of Maxwellian self-consistency in distribution of ions and electrons, requiring extensive computer based calculations for solution. A very simple approximation, ignoring the effect of the potential, gives the radial electron velocity at any radius as just:

$$v_{er}(r) = \sqrt{v_{r0}^2 \langle r \rangle^2 - v_{to}^2} \quad (1c)$$

where $\sim v_{ro} = \sim v_{er}(R)$ and $\sim v_{to} = \sim v_{e\perp}(R)$ are mean radial and transverse speeds at the surface in the recirculating flow. Since conservation of transverse momentum in the potential well requires $\sim v_{e\perp}(r) = \sim v_{to}/\langle r \rangle$, the radial electron speed in this crude model is:

$$v_{er}(r) = (\langle r \rangle v_{r0}) \sqrt{1 - \left(\frac{v_{t0}}{v_{r0}}\right)^2 \left(\frac{1}{\langle r \rangle^4}\right)} \quad (2)$$

For monoenergetic injection electrons, the rapid variation of electron speed obtains only for the region in which $I > \langle r \rangle^2 >> (\sim v_{to}/\sim v_{ro})$. At $(r/R) = \langle r_f \rangle = (\sim v_{to}/\sim v_{ro})^{0.5}$ all radial electron flow due to electron inertial forces alone ceases. From this position to smaller radii, the electrons no longer drive a negative potential well, and the well is not as deep as if the electrons had no transverse momentum and could convert all of their radial energy into electrostatic potential energy. This result for $\langle r_f \rangle$ approximates the correct result, including the electrostatic potential, for the case in which the transverse energy of electrons is comparable to or larger than their radial kinetic energy near the surface.

Inside this radius, the ions move without further acceleration, but continue inward with their large momentum, dragging electrons with them to provide the required near-neutralization of charge. Electron drag takes energy from the ions, but this energy loss is small due to the small electron mass. Thus, the ions continue to converge along their previous paths of motion, but no longer under an attractive central force field. Rather, their radial motion slows down due to virtual anode buildup and to conservation of ion transverse momentum. This latter effect finally sets the limit on ion particle convergence in any system of practical interest. Slowing down due to virtual anode buildup results in a central density increase scaling faster than the $1/r^2$ scaling that applies in the midrange of well radial position.

This scaling can be estimated crudely by considering the case in which the ion energy distribution function in the core is not broadened or distorted significantly by in-core collisions, so that the ions return to the radial position of their injection ($r_i < R$) in each recirculation with only the energy with which they were injected, or dropped, into the well. Then, again ignoring potential shape, the radial speed $\sim v_{ir}(r)$ at any position is given by:

$$(v_{ir}\langle r \rangle)^2 = \left\{[v_{ir}(R)]^2 + [v_{ir}(r_0)]^2\right\} - \langle r \rangle^2 \left\{[v_{ir}(r_0)]^2 + [v_{it}(R)]^2 \left\langle \frac{1}{r} \right\rangle^4\right\} \quad (3)$$

The injection radius should be sufficiently inside the system magnetic surface boundary so that ions are introduced away from the most bumpy region of the surface field. Then, if the polyhedral field is configured to fall off rapidly with decreasing radius, the maximum transverse ion velocity that can be produced by repeated reflections in the magnetic field can be limited to a few times $(1/\alpha)$ that of the radial speed at ion injection, $\sim v_{i\perp}(R) = \sim v_{ir}(R)/\alpha$. With this constraint on tangential

speed, the ion convergence limit can be shown to be reached at approximately:

$$\langle r \rangle^2 = \frac{(E_{i0} / E_w)}{\alpha^2} \qquad (3b)$$

where E_{io} is the (radial) ion injection energy. Thus, for E_{io} = 10 eV, α = 0.3, and E_w = 10^5 eV, the convergence limit ratio is $\langle r_o \rangle \approx 3 \times 10^{-2}$.

This discussion is too simple for the real case, but it serves to show the general nature of the effects anticipated and the limits for near-optimum conditions. In a real system, the angular energies and momenta of both particle streams exhibit a spread and distribution, the effects of scattering reflection from the polyhedral magnetic fields are governed by the actual, three dimensional shape of the internal B and E fields, and the E field distribution may, itself, be determined by turbulence, mixing, or other unstable redistributions of the plasma ions and electrons as they move through mid-range radii of the device. In such conditions, the ion orbits and their spreading must be calculated by single-particle codes in a realistic geometry with the actual field structure to obtain a good estimate of the minimum convergence ratio possible in any given system. Having such estimates, it is then possible to model the ion density convergence by simpler algorithms.

For purposes of illustration, it is often sufficient to assume that the particle densities vary radially in a power-law fashion as:

$$n_e(r) = \frac{n_{e0}}{\langle r \rangle^m} \qquad (3c)$$

and

$$n_i(r) = n_{im}[\langle r_0 / r \rangle^m] \qquad (3d)$$

where the exponent m is taken as $2 \le m \le 3$, and n_{eo} and n_{im} are surface and core densities of electrons and ions, respectively. To assess the effect on well depth of this variation, it is necessary to integrate the expressions for density variation over $r_o < r < R$ by Poisson's equation, using the more complex velocity-dependent forms for density distributions in the regions inside and outside the electron virtual cathode or "stagnation" radius r_f. With these, the well depth is found as a function of system size, surface electron charge density, and the particle angular beam spread. The resulting formula can be approximated for $\langle r_f \rangle > 0.3$, $\langle r_o \rangle < 0.1$ by:

$$E_w = (2\pi R^2)(n_{e0} e)\left[\frac{F1\langle r_f \rangle}{r_f} - 1\right]\left[\ln\left(\frac{1}{r_0}\right)\right] \qquad (4)$$

where $F1\langle r_f \rangle = [2 - \langle r_f \rangle^2]^{0.5}$. If $\langle r_f \rangle = 1$, the well depth is zero, as expected. From this, the surface electron density becomes:

$$n_{e0} = \frac{E_w}{2\pi e R^2}\left[\frac{F1\langle r_f \rangle}{\langle r_f \rangle} - 1\right]\left[\ln\left(\frac{1}{\langle r_0 \rangle}\right)\right] \qquad (5)$$

Comparison of this with Eq. (1) for assumed constant net charge density shows that the effect of radial inertial convergence of the particles in this dynamic system is to decrease the (net) electron charge density required in the surface region for the generation of a specified well depth by a factor of $\rfloor[3 \ln(1/\langle r_o \rangle)] \times [(F1\langle r_f \rangle/\langle r_f \rangle) - 1]$.

Efficient well generation requires small $\langle r_f \rangle$; unfortunately, surface field reflection can produce large transverse momentum in the electrons. Here $\langle r_f \rangle$ is taken as $\langle r_f \rangle^2 = 0.2$, corresponding to electron angular energy one-fifth that of the radial motion at the surface radius. In systems of interest, the desired ion convergence ratio is $1/\langle r_o \rangle > 100$. For $\langle r_o \rangle = 10^{-2}$, for example, the density reduction factor is ~26 for electron spreading such that $\langle r_f \rangle = 0.45$. This means that electron losses through the surface magnetic field and polyhedral cusp regions will be 26 times less than would be estimated by the simple (but incorrect) constant-charge-density model. Thus, electron injection power requirements will also be much less than otherwise.

III.B. MHO and Aspherical Deformation Stability

The polyhedral field configurations of interest in this paper are all constrained by the requirement that an even number of faces surround every vertex of the system geometry. Under this condition, current carriers along the edges, or wound around on each of the faces, will result only in point (or polar) magnetic cusps; there will not be any line cusps in such systems.

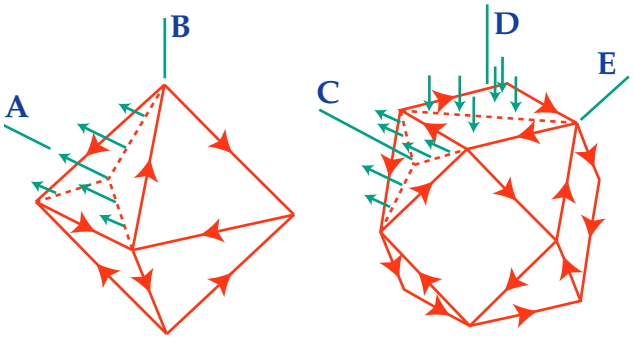

Figure 4 — Octahedral and truncated cube polyhedral geometries, showing face-center magnetic fields (A,C,D), field direction on face-symmetry lines, and axes of null field (B,E). Arrows on polyhedron edges indicate direction of current flow in edge conductors to product desired fields.[14]

Figure 4, taken from Keller and Jones,[14] shows two examples of such geometries. An inherent feature of these geometries is that all such systems are MHO stable to surface perturbations of confined plasma.[18]

In their early work, Elmore et al.[12] posited the instability of purely electrostatically confined (i.e., no external *B* fields) ensembles of ions and electrons for the case in which the ions had a radially Maxwellian energy (and velocity) distribution about a mean energy <*T*> at ~0.2 of the well depth. For this model, they showed that extremely large ion currents were needed for net system gain and that the required high ion densities led to instability of the confinement. For the polyhedral system here, with all particles much more nearly radially monoenergetic in contrast with the radial Maxwellian model, their condition for net power operation (system gain, $G > 1$) leads to a constraint on the electron injection current, which is roughly:

$$I_{e-} \geq 1.6x10^{12}\,\frac{r_0 T_e \sqrt{E_w}}{G_j^2} \qquad (6)$$

where:

I_{e^-} = electron injection current (A)

r_o = radius of the reaction core (cm)

T_e = equivalent energy spread or "temperature" of the recirculating electrons (keV)

G_j = electron current recirculation ratio
= total circulating electron current/injected current.

For a typical case of interest, take T_e = 2.0 keV, E_w = 100 keV, G_j = 2.0 x 10^5, and r_o = 0.6 cm. The electron injection current required is $I_{e^-} \geq$ 500 A, and the injected power is P_{e^-} = 5.0 x 10^7 W = 50 MW(electric). The recirculating current here is only ~10^{-7} of the current required in the system of Reference 12. Furthermore, solving Poisson's equation for monoenergetic ions, it is found that there is no static bound set on ion density, save that $(n_i/n_e) < 1$; larger n_e allows larger n_i.

This difference in system configuration and constraints carries over to the issue of stability. The virial theorem argument given in Reference 12 fails since the surface integral invoked always vanishes because the magnetic fields prevent particle displacements at the surface. Non-spherical modes within the plasma that do not correspond to the field symmetry are damped, thus restricting allowable internal displacements, and microturbulent damping of very short waves forces these to intermediate wavelengths. Thus, only long-wavelength, (a)spherically (or polyhedrally) symmetric modes are allowed, and these are frozen at the field boundary. The existence of such modes may act to limit transverse momentum generation in recirculating ion flow.

Another approach to the gross instability issue was given by Furth,[13] who studied a pure electrostatic system with displacements induced by an azimuthal perturbation magnetic field. Limiting perturbation speeds by dielectric field limits on ion speed and taking ion flow in an assumed parabolic potential well reduces the instability criterion to:

$$\langle n_{e,i} \rangle < 10^{14} \left(\frac{R}{r^3}\right) \sqrt{\frac{m_i}{m_e}} \left(\frac{1}{cm^3}\right) \qquad (7)$$

where:

R = system radius

r = internal radial position within which are found all of the perturbing particles at uniform density.

If this constraint were to apply (i.e., all magnetic fields were removed), it would not significantly limit the potential power generation rate of such a device, if the convergence ratio can be made small enough. This can be seen from the power equation, evaluated at particle density from the limit condition above:

$$P_f = E_f (n^2)(\sigma v) V \qquad (7b)$$

where:

E_f = reaction energy

σ = fusion cross section

$V = (4\pi/3)(r^3)$ = reaction volume

For example, take R = 100 cm and assume that ion density is constant in the reacting region ($r < r_o$). For use of p-^{11}B, m_p/m_e = 1850 and E_f = 8.7 MeV. At a well depth of E_w = 4 x 10^5 eV, the reaction cross section is (σ = 0.4 x 10^{-24} cm^2 (0.4 b) and v = 6.2 x 10^8 cm/s. With R = 100 cm and a convergence ratio $\langle r_o \rangle = 10^{-2}$, the limiting ion density and power output are 4.3 x 10^{17} /cm^3 and 170 MW, respectively. Since all the power in this system comes from a small dense central core, it is evident that even under the limiting density condition the power generation still can be very large.

An estimate can also be made of the effect of the surface fields on suppression of this prolation instability. The driving force for gross motion is the magnetic pressure surrounding the prolating sphere due to the magnetic fields generated by the perturbation axial flow of charged particles. The displacement speed cannot exceed the ion speed (dielectric coupling); thus, the maximum perturbation current and field due to a displacement involving N_{tot} particles can be estimated as:

$$I_z = \frac{\delta v(N_{tot})}{6.28x10^{18}} \qquad (7c)$$

and

$$B_p = \frac{0.4 I_z}{R} \quad (7d)$$

where

I_z = maximum perturbation current (A)

B_p = maximum perturbation field

δv = perturbation speed (cm/s).

The magnetic field perturbation energy density due to this axial current is:

$$\frac{B_p^2}{8\pi} = 4.06x10^{-39}\left[\frac{\delta v(N_{tot})}{R}\right]^2 \left(\frac{erg}{cm^3}\right) \quad (8)$$

The electrostatic confining energy density is just $(E^2/8\pi)$, where the electric field E can be approximated by $2E_w/R$; thus, stability is ensured for $B_p^2 < E^2 = 4(E_w/R)^2$. From this, stability requires that:

$$N_{tot} < 6x10^{19}\left(\frac{E_w}{\delta v}\right) \quad (9)$$

Taking the perturbation speed to be that of (low-energy) surface ions at $\delta v = 10^{-3} v_{imax}$ and a well depth of E_w = 100 keV gives the limiting number of participating particles as $N_{tot} < 3 \times 10^{16}$, independent of the system size R. For this number of particles participating in the prolate motion, the maximum perturbation field that can be produced in a system of size R = 100 cm is only B_p = 4 G. In all practical cases, the externally supplied polyhedral surface field strength B_e is ≥ 1 kG. Thus, this hypothetical disturbance cannot be sustained or initiated; it is prohibited by the surface fields previously ignored.

In the previous estimation, the unstable particle number is independent of R; thus, prolate perturbations may occur over smaller radial regions at higher density. Here the local perturbation field B_p is larger and the stabilizing polyhedral field B_e is less. The local E field slowly decreases as $r < R$, going to zero at r = 0. At some radius r_b, the two fields (B_p, B_e) will balance. Within this radius, the prolate deformation cannot be stabilized by the external field alone. For an externally imposed field that varies as $B_e(r) = B_o(r/R)^3$, for $B_e > B_p$ to be satisfied it is necessary that:

$$B_0\left(\frac{r}{R}\right)^3 > \frac{0.4\delta v(N_{tot})}{(r_b)6.28x10^{18}} \quad (10)$$

Taking $N_{tot} = 6 \times 10^{19}(E_w/\delta v)$, determined above, gives the field required as:

$$B_0 > \left(\frac{4E_w}{R}\right)\left(\frac{R}{r_b}\right)^4 \quad (11)$$

For E_w = 100 keV and R = 100 cm, this gives $B_o > 4(R/r_b)^4$. The surface field required for stability down to a radius of (r_b/R) = 0.25, for example, is about $B_o \sim$ 1000 G (1 kG). A different radial dependence of the B field will yield other numerical conditions, but this illustrates the general situation.

Finally, there is another source of stabilizing energy that acts to inhibit and/or prevent aspherical deformations throughout the system, especially at small radii. As the ions fall into the well, they acquire the energy of the well depth at their radial position. The well acts as a momentum transformer, using electron injection energy to create ions with large momentum at small radii. The ion flow energy and momentum is very large and highly spherically symmetric. This can act as a powerful stabilizing energy source against aspherical perturbations, by means of the transverse and radial dynamic pressures represented by the ion momentum acting on streaming particle motion, to suppress or prevent deformations from sphericity.

III.C. Electron Collisional Transport and Particle-Cusp Losses

Electron losses can occur by electron-electron collisional transport across the bounding surface field region, with losses characterized by a transport coefficient K in the usual formula $q_{te} = K\Downarrow_\perp(E_w)$ for electron energy flux q_{te} across the field. Electrons are reflected by turning through their gyromagnetic radius in the surface field. At this radius, they have their maximum energy of injection $E_{eo} > E_w$. Electron collisions in the gradient of electron density ensure that a flux of electrons (and consequent energy) is transported across the field. However, the classical transverse collisional transport coefficient $K_\perp$ for this process is too small to lead to any significant power loss from the device.

In contrast, the transport coefficient K_x is very large for surface-parallel electron motion due to electron gyration around the field lines. This flow consists of a current sheet circulating around the axis of each of the magnetic polar cusps, resulting in diamagnetic reduction of the local strength of the B field. It is in a direction $\boldsymbol{b} \times \Downarrow E_w$ ($\boldsymbol{b}$ is the unit vector along the B field) and is not a loss, but a circulatory $(v \times B) \times B$ drift. Some fraction of this gross directed flow leads to collisional enhancement of the transverse losses by collisions with particles moving normal to the field surface.

This effect may be accounted for as the geometric mean of the transverse and cross-field transport coefficients to give an effective coefficient (K) for diffusion/transport losses through the magnetic surface. Standard equations[19] for these transport coefficients give this mean coefficient as:

$$\langle K \rangle = \sqrt{K_t K_x} = \frac{3.33x10^{19}\langle Q \rangle^{1.5}}{\sqrt{E_w}}\left(\frac{1}{cm \bullet \sec}\right) \quad (12)$$

where:

$\langle Q \rangle = (j_o G_j / B)$

j_o = electron injection current density (A/cm²)

G_j = current recirculation ratio.

The total surface electron flux is given by $j_o G_j = (n_e v_e)/6.28 \times 10^{18}$, where v_e is electron speed at injection energy ($5.925 \times 10^7 E_w^{0.5}$ cm/s).

The electron energy gradient $\Downarrow_L(E_w)$ can be written approximately as $\Downarrow_L(E_w) = E_w/(\delta R) = E_w/(\delta L)R$, which defines the fractional thickness of the effective surface field region as $(\delta L) = (\delta R/R)$. Total power loss by this mechanism is $\langle P \rangle = q_{te}(4\pi R^2)$. Combining the terms gives this power flow as:

$$\langle P \rangle = 66.9 \frac{\langle Q \rangle^{1.5}\sqrt{E_w}R}{\delta t}(watts) \quad (13)$$

Take the current density $j_o = 10^{-4}$ A/cm², $G_j = 10^5$, the field as $B = 10^3$ G, $R = 100$ cm, $E_w = 10^5$ eV, and $(\delta L) = 5 \times 10^{-2}$. For this case, the above formulas give $\langle K \rangle = 2 \times 10^{13}$/cm•s, and $\langle P \rangle = 5.68 \times 10^4$ W = 56.8 kW, which is small compared with power generation rates of interest. Comparison of this with classical transport and its enhancement by microturbulent oscillatory phenomena (Bohm diffusion[20]) shows this as larger than classical by a factor of the order of 4×10^5, or very nearly the same as that for Bohm diffusion.

Another mechanism for the loss of electrons and energy from the system is escape through the polar magnetic cusps that surround the confined core volume. The escape path is from that area of the cusp through which electrons can move radially outward from within the system without being reflected by magnetic momentum conservation in the cusp magnetic field gradient. This is approximated by[21,22,23] the area of a circle whose radius is the gyromagnetic radius r_e of the electron at its energy in the magnetic field of the cusp. This leakage radius applies for the case, valid here, of trapped electrons in a non-neutral plasma system and not for the confinement of neutral plasma, which can escape through a leakage path width comparable to the geometric mean of the ion and electron gyro radii ($r_{e,i}$) in the cusp field. Note also that $r_i < r_e$ at conditions of interest.

The fraction f_c of electrons escaping through cusps at any given time is simply the ratio of the total area of gyroradius holes to the area of the surface of the system; thus:

$$f_c = \left(\frac{N}{4}\right)\left(\frac{r_e}{R}\right)^2 \quad (13a)$$

where N is the number of cusps used in the system. For a system in which such losses through cusps dominate all other electron consumption mechanisms, the maximum possible recirculation ratio is $G_{jm} = 1/f_c$. To evaluate the loss fraction, take the gyroradius as √2 times the usual formula[14] because the electrons here are in directed motion rather than in thermal equilibrium, as in the conventional case. The electron loss fraction then becomes:

$$f_c = 2.83\left(\frac{E_w}{B^2}\right)\left(\frac{N}{R^2}\right) \quad (14)$$

The total electron cusp power losses are equal to this factor multiplied by the total power carried in surface current of electrons at radius R in the system, which is equal to the injected electron density averaged over the sphere, multiplied by the surface area, the electron current recirculation ratio G_j, and the energy carried per electron. This leads to:

$$P_b = 35.9\frac{(NE_w^2)(j_0 G_j)}{B^2} = 35.9\left(\frac{NE_w^2}{B}\right)\langle Q \rangle (watts) \quad (15)$$

where:

j_o = average injected surface current density of electrons

G_j = current recirculation ratio

$\langle Q \rangle = (j_o G_j/B)$.

The parameters j_o and G_j are not independent of the other variables in the equations but are related to them by various constraint or defining equations. As previously, the maximum possible value for the current recirculation ratio is given by:

$$G_{jm} = \frac{1}{f_c} = 0.353\frac{(RB)^2}{NE_w} \quad (15b)$$

The electron injection power can never be less than the cusp loss power; thus:

$$P_{inj} = j_0 E_w (4\pi R^2) \geq P_b \quad (15c)$$

from which a constraint on j_o can be found for any values of other parameters. To show the range required for high values of G_j, consider an octahedral system, $N = 8$, with a radius $R = 100$ cm, well depth of $E_w = 10^5$ eV, and a field of $B = 2 \times 10^3$ G. For these values, the upper limit current gain factor is $G_{jm} = 1.76 \times 10^4$. To reach $G_{jm} > 10^5$, the field in this system must be $B > 4.76 \times 10^3$ G. For operation at $j_o = 10^{-3}$ A/cm², the injection (and cusp loss) power would then be $P_{inj} = P_b = 12.6$ MW.

IV. Positive Ion Trapping, Stability and Radiation Losses

IV.A. Convergent Ion Flow. Momentum Transformation. and Pressure Balance

At the surface, the electron energy and momentum are highest while the ion energy and radial momentum are least. The electron radial energy and momentum are least and the ion radial and/or transverse momentum and energy are highest near the device center. The device thus functions as a "momentum transformer" in which the ion dynamic pressure in the central core region is much greater than the electron dynamic pressure at the surface due to electron reflection by the polyhedral magnetic fields.

This can be assessed by estimating the variation of ion and electron densities and speeds with radial position in the potential well. The local net charge density is determined by the exchange of particle kinetic energy with potential energy, according to the instant solution of Poisson's and the energy/momentum and particle flux conservation equations. Analytic solutions are complicated by the requirement of Maxwellian self-consistency throughout the system, even in the absence of energy-exchanging collisions, and such collisional terms are not included in these fluid models. Even these require use of numerical methods and computer calculations; some have been carried out by Ensley et al.[24] with an approximate 1.5-dimensional Vlasov-Maxwell code. Other numerical simulations were performed by Goplen[25] using the PIC code MAGIC on Cray computers. Results of these computations showed that ion density convergence could be modeled approximately for simple analyses by assuming ion and electron density to vary as a power of the radial position; $n_\sim(r) = n_{\sim o}/\langle r\rangle^{m_\sim}$, with $2 < m_\sim < 3$, as before.

The momentum transformation property is best illustrated by considering the dynamic pressures at the system center and boundary due to particle motion and reflection in these regions. As already noted, because of the difference in the ratio of energy to momentum of the electrons and ions, the central core dynamic pressure at ion speeds is much larger than the external surface dynamic pressure resulting from electron reflection. This latter is $p_{e^-} = (n_{\sim eo} m_\sim v_e)/2$ at $r = R$; the former is $p_{i+} = (n_{\sim im} m_{\sim i} v_e)/2$ at $r = r_o$. Here $n_{\sim eo}$ and $n_{\sim im}$ are the electron and ion densities at the effective surface and central core radius, respectively. For a well depth taken as equal to the electron injection energy, the particle energies are related by:

$$E_w = \frac{m_e v_e^2}{2}(at\ R) = \frac{m_i v_i^2}{2}(at\ r_0) \qquad (15d)$$

Thus, the ratio of dynamic pressures becomes:

$$\frac{p_{i+}}{p_{e-}} = \langle p_{ie} \rangle = \left[\frac{n_i(r_0)}{n_e(R)}\right] = \frac{n_{im}}{n_{e0}} \qquad (16)$$

Since the charge densities must be very nearly equal in the system center, it follows from:

$$n_{e0} \approx [n_e(r_0)][\langle r_0 \rangle^m] \approx [n_i(r_0)][\langle r_0 \rangle^m] \qquad (16b)$$

that the pressure ratio is $\langle p_{ie}\rangle \approx 1/\langle r_o\rangle^{m_\sim}$. If $m_\sim = 2$ and $\langle r_o\rangle = 10^{-2}$, for example, this gives $\langle p_{ie}\rangle = 10^{-4}$, while $\langle p_{ie}\rangle \approx 10^8$ with $m_\sim = 3$, $\langle r_o\rangle = 10^{-3}$. It is clear that the ratio of equivalent central-to-surface pressures is very large for any parameters of interest. The internal ion dynamic pressure can be much larger than the electron dynamic pressure sustained by the external B field. This confining field need not support the pressure in the reacting core, only that of the electrons that make the negative well.

The surface pressure balance is:

$$p_{e-} = n_e E_w = \beta_e \left(\frac{B_0^2}{8\pi}\right) \qquad (16c)$$

where

β_e = magnetic pressure "efficiency" factor ($\beta_e \le 1$)

$n_{\sim e}$ = surface density of recirculating electrons.

The surface field required to support the dynamic pressure is then:

$$B_0^2 = \left(\frac{8\pi}{B_e}\right) n_{e0} E_w \qquad (16d)$$

or

$$B_0^2 = \left(\frac{8\pi}{B_e}\right)(G_j j_{e0})\sqrt{\frac{m_e E_w}{2}} \qquad (16e)$$

where j_{eo} is the surface average electron injection current. This then becomes:

$$B_0^2 = 4.236\frac{G_j j_{e0}\sqrt{E_w}}{B_e} \qquad (17)$$

For example, if $E_w = 10^5$ eV and $n_{\sim eo} = 10^{10}$/cm^3, then the field is given from $\beta_e(B_o)^2 = 4.01 \times 10^4$ dyn/cm^2. Assuming a very conservative value of $\beta_e = 0.04$, a surface field strength of only $B_o = 10^3$ G = 1 kG is required. This system has $\langle G_j j_{eo}\rangle = 30.0$ A/cm^2 of circulating current density. Note that the absolute minimum surface field (for $\beta_e = 1.0$) needed here is only $B_o \approx 200$ G. With a convergence ratio of $\langle r_o\rangle = 10^{-3}$ and a density scaling exponent of $m_\sim = 2$, this ($\beta_e = 0.04$) field is "equivalent" to a

central field strength of $B(r_o)$ = 10⁶ G = 1 MG. Note that no "physical" magnetic field of this sort is found in the central region (the external field falls typically as $\langle r \rangle^3$); this equivalent field is simply illustrative of the central region dynamic pressure associated with momentum transformation as exhibited in the radial velocity of the ions.

On an energy basis, this is entirely consistent with the observation that the central confinement energy region must contain energy equal to or less than that of the external dynamic pressure energy density over the total spherical volume. Thus p_{i+} (*center*)$r_o^3 \leq p_{e^-}$ (*surface*)R^3, which is identically true for the scaling used here, with $m \backsim < 3$. The net result of this inertial flow system is that confinement energy is localized only to the region where it is needed. The surface fields ($r = R$) see only this energy averaged over the whole system volume, while the central particles see the maximum pressure over the reacting volume at $r = r_o$.

IV.B. Electrostatic Waves, Dynamic Pressure. and Core Stability

In early studies of conditions for energy exchange between interpenetrating streams of charged particles, both Klimontovich[26] and Furth[13] showed conditions for the onset of instability momentum coupling through self-excitation of oscillations between counterstreaming currents or between a beam going into a plasma. In general, both found that an initial perturbation would generate its own velocity correction so as to reverse field growth along the beam direction, as long as the densities allow coherent effects to take place. It is only when the particle densities reach sufficiently large values that collisional effects begin to dominate the motion and convergence ceases (i.e., as $r \rightarrow r_o$) that wave generation can occur. At this point, the waves themselves then create an electrostatic "envelope" within which collisional processes dominate and suppress further wave growth. Such central electrostatic structures then act as the boundary for momentum exchange and pressure balance on the core region.

The general condition for onset of electrostatic waves was shown[23] to be:

$$\frac{n_b}{n_p} > \left(\frac{v_b}{v_{th}}\right) \exp\left\{-0.5\left[1+\left(\frac{v_b}{v_{th}}\right)^2\right]\right\} \quad (18)$$

for the most rapidly growing wave with:

$$\lambda_w = \frac{1}{k} = \lambda_d\left(\frac{v_b}{v_{th}}\right) = \frac{v_b}{\omega_p} \quad (18b)$$

where:

$\lambda_d = (E_{th}/4\pi n e^2)^{1/2}$ = Debye shielding length

$\omega_p = (4\pi n e^2/m \backsim)^{1/2}$ = plasma frequency

v_b, v_{th} = velocity of beam and thermal electrons, respectively.

Therefore, instability starts as the condition $E_{th}/n \backsim < 10^{-12}$ eV/cm³ is reached. This can happen only for small thermal dispersion of the electrons at large densities, a state achieved only near the center of the system. These general results and conclusions have been verified in other cases[27] of increasing particle density with increasing current density. They can be summarized as follows:

1. Counter-streaming electrostatic wave generation by electron and ion instability motion is possible only where instability wavelengths are small enough relative to field gradients to permit coherency. This is not generally the case in the outer regions of the spherically convergent confinement system, where ion and electron densities are small, electron energy is high, and ion energy is low.
2. Spherical electrostatic waves can be initiated at conditions of large density of electrons and ions, where electron energy is low and ion energy (temperature) is high and where instability wavelengths are small relative to field gradients.
3. These latter conditions are found in or near the central core region of the system, where convergence is high. Here the wave structures generated can act as a momentum transfer mechanism between ions outside the core and particles within it, thus providing a momentum transformation between externally injected electrons and internally reflected ions.

The nature and magnitude of this momentum transformation have already been examined and were shown to yield a dynamic pressure in the central core region that varies as $(R/r)^{m \backsim}$ (where $2 < m \backsim < 3$) times the electron dynamic pressure on the external magnetic field. This dynamic pressure arises from recirculating power flow in the system. Study of operating conditions for useful systems shows that this flow can be several thousand times larger than the fusion power that the system will generate. Furthermore, this very large power flow appears as tangentially isotropic azimuthal motion in the core region, somewhat in the fashion of a spherically symmetric "vortex" flow around the well center.

This fact suggests that neither small-scale local disturbances nor the generation of fusion power at useful levels within the system can appear to the system dynamics and energetics as a significant perturbation on the already very large power flow within it. Thus the generation of fusion power is unlikely to be a destabilizing mechanism; if the large power flows inherent in the de-

vice can be kept stable without fusion, then the addition of fusion generation will have little effect. It also suggests that no instability mechanism can produce gross asymmetric instabilities, nor can instabilities be initiated microscopically that lead to unconstrained amplitudes of unstable growth sustained against the stable spherical quasi-vortex motion of ions near the center. Thus it appears that dynamic ion momentum transformation forces can stabilize all of the converged core region against gross perturbations.

IV.C. Synchrotron Radiation and Bremsstrahlung losses

Synchrotron losses occur in any system of charged particles in magnetic fields. Electrons contribute nearly all of the synchrotron radiation because their acceleration is larger by the ratio of ion to electron masses. In the system here, furthermore, the ions are at low energy where the field is high (at $r = R$), while the electrons are at their highest energy at that point.

These losses are given by the usual formula (19) for the power density radiated by electrons moving in a magnetic field as:

$$P_{syn}(r) = 1.24x10^{-27}[n_e(r)][E_e(r)][B(r)]^2\left(\frac{W}{cm^3}\right) \quad (19)$$

for cgs units. This has been modified (increased by a factor of 2) for non-thermal electrons in the surface field region. The total synchrotron power radiated is found by integration over the volume, using appropriate algorithms for variation of the parameters involved. The electron energy is assumed to scale parabolically, $E_e(r) = E_w(r/R)^2$, while the density is taken as $n_e(r) = (n_{eo}G_j)(R/r)^2$, a conservative assumption that will lead to an overestimate of synchrotron losses. Finally, the magnetic field is taken here to scale with radial position in the system approximately as $B(r) = B_o(r/R)^3$. With these, integration gives the synchrotron power as:

$$P_{syn} = 1.73x10^{-27}(n_{e0}G_j)E_w)B_0^2R^3(watts) \quad (20)$$

or

$$P_{syv} = 1.82x10^{-16}(j_0G_j)\sqrt{E_w}B_0^2R^3(watts) \quad (21)$$

In Eq. 21, the identity $(n_{eo}v_{eo}) = 6.28 \times 10^{18} j_o$ for injection current density and particle flow [with $v_{eo} = (2E_w/m_e)^{1/2}$], is used to introduce the parameter j_o through $n_{eo} = 1.05 \times 10^{11}(j_o/E_w^{0.5})$.

As an example, consider a system with $j_o = 10^{-3}$ A/cm^2, a current gain of $G_j = 10^5$, $B_o = 5 \times 10^3$ G (larger than the limiting field 4.76×10^3 G for the assumed value of G_j), $E_w = 10^5$ eV, and $R = 100$ cm. For these values, the total synchrotron radiation loss is only $P_{syn} = 144$ W. No other reasonable parametric combination of values can raise this to a level of significance for the system here, and it is henceforth neglected.

Whenever charged particles are in proximity and undergoing long-range interactions and small-angle collisions, the lightest particles are most accelerated by these collisions. This acceleration results in the emission of electromagnetic radiation (bremsstrahlung) by the accelerated particles. This radiative output power density from electron-ion collisions in a mixture of nearly equal numbers of ions and electrons at electron temperature T_e at density $n_e = n_i = n_{ei}$ is given by: [19]

$$q_{br} = 1.69x10^{-32}(n_{ei}^2Z^2)\sqrt{T_e}\left(\frac{W}{cm^3}\right) \quad (22)$$

where Z^2 is the mean-square charge of the ions. A similar equation can be written for ion-ion bremsstrahlung, with a Z^4 term added.

At $r = r_o$, the electron energy (temperature, for purposes of calculating bremsstrahlung) is much less than the ion temperature (energy), $T_e \leq 10^{-2} T_i$, and the ion temperature is at its maximum value, $kT_i = E_w$. Conversely, at the surface ($r = R$), the electron energy is highest at $T_e = E_w$, and the ion energy is lowest, $E_i = E_{io}$ = ion injection energy. The relative importance of each type of collision process will thus vary across the machine.

Consider an electron-ion mixture of $p^+ + {}^6Li^+$, with $\langle Z^2 \rangle = 5$ (average for the mixture). The ratio $\langle q_{br} \rangle$ of ion-ion bremsstrahlung to electron-ion radiation is $\langle q_{br} \rangle \leq 3.9 \times 10^{-3}$ at $r = r_o$, and $\langle q_{br} \rangle \leq 3.9 \times 10^{-6}$ at $r = R$. In making these calculations, the central ($r \rightarrow 0$) electron temperature was assumed to be much less than the core ion temperature, $T_e \leq 10^{-2} T_i$, and the surface ($r = R$) ion temperature (energy) was taken as much less than the electron injection energy, $T_i \leq 10^{-4} T_e$. For these conditions, which correspond to typical system operation, the ion-ion bremsstrahlung is everywhere negligible compared to electron-ion collision radiation.

The electron-ion radiation is largest at the system center, even though the electron temperature is least because the densities are high in this region. There is a lower limit on the temperature that may be used in such an estimate for radiation from the core — the temperature of either particle that yields the largest particle speed. If the electron speed is less than the ion speed, then the ion speed should be chosen for the collision process, and an equivalent electron temperature (to give this speed) be used in the formula. If the electron speed is largest, the electron temperature should be used directly.

The electron speed tends to be comparable to the core ion speed, since the electrons follow the ions into the

core as these converge toward the center. In a sense, ion drag is the force that brings electrons into the core region. Therefore, it is reasonable to take core region electron speed as equal to that of the lightest ion component, for which the electron energy is less than the well depth simply by the ratio of the electron to ion masses. Equal speeds require that the electron energy be of the order of 10^{-4} the ion energy, or at $10^{-4}E_w$ (typically 10 eV). This seems impractical to attain even in the best of wells. For purposes of calculation, assume that $E_e = 10^{-3} E_i$ at $r = r_o$. Thus, electron speed at the well bottom is of the order of 2 to 3 times the ion speed for ions from *p* to *T*.

Of most interest is the relative power density of bremsstrahlung radiation to that of fusion power production in the core. This latter is:

$$q_{fus} = (n_i^2)(\sigma_f v_i) E_f b_{ij} \quad (23)$$

where:

b_{ij} = 0.5 for identical particles and 0.25 for unlike particles

E_f = energy per fusion reaction (MeV)

σ_f = reaction cross section (b)

Taking the ratio of these two gives:

$$\frac{q_{br}}{q_{fus}} = 2.36x10^{-3} \frac{Z^2 \sqrt{M_i}}{\sigma_f E_f (b_{ij})} \quad (24)$$

where M_i is the normalized reduced mass of the ions, $M_i = m_1 m_2/(m_1 + m_2)(m_p)$, where m_p is proton mass.

The fusion reaction cross section is a strong function of ion energy, increasing rapidly with increasing energy over the range of interest. Therefore, it is evident that there is a well depth for any given fuels above which fusion exceeds bremsstrahlung power density. This critical level determines the minimum well depth at which the concept can function as a useful net power device. This can be estimated from the reaction energies and cross-section variation with energy of various candidate fusion fuels, for collisions constrained to the CM frame coincident with the CG of the device.

Using standard tables and the graphical representations in Figure 5 for fusion reaction cross-section variation with interaction energy, limiting minimum well depths for break-even in the core were found to be roughly as given in Table 1 for various fuels. Well depths must be greater than these limiting values to ensure significantly larger power generation by fusion than by radiation. These values are reduced if the electron temperature in the core are less than assumed above. For example, for equal electron and ion speeds, the effective temperature for radiation purposes is reduced by a factor of ~4 and the (q_{br}/q_{fus}) ratio by a factor of 2. This results in a reduction of limit well depths to 0.7 to 0.9 of those given above. Conversely, higher core electron energies raise the critical well depths.

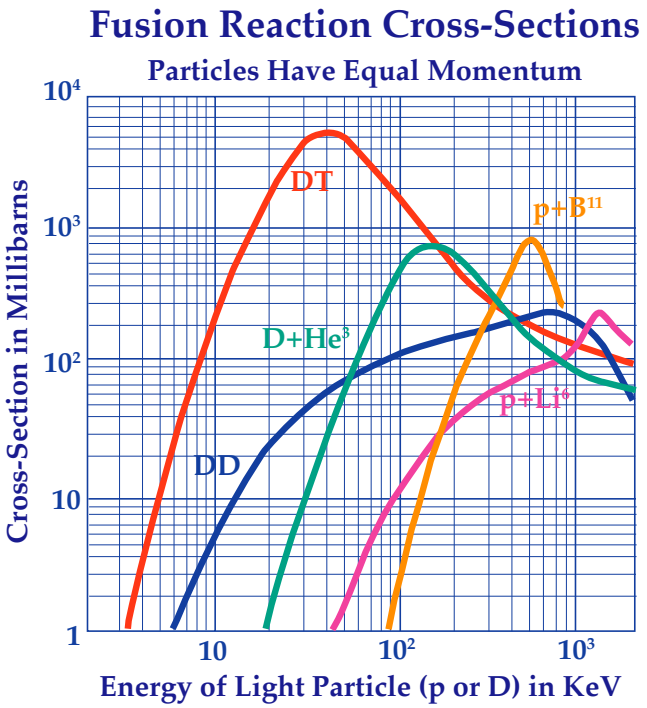

Figure 5 — Mono-energetic fusion reaction cross sections in CM coordinate frame for several candidate fuels.[2]

Table 1 — Minimum Well Depth for Equal Bremsstrahlung and Fusion Power Densities

Fuel	Energy, E_f (MeV)	Well Depth E_w (keV)
D-T	17.6	1.7
D-^{3}He	18.3	19.5
p-^{6}Li	4.0	100
p-^{11}B	8.7	144

V. Reaction Power Generation and Collisional Effects

V.A. Reaction Rate Density and Power Generation

The total fusion power output is given by the integral of the fusion reaction power density over the volume of the system:

$$P_f = \int_0^R dr(4\pi r^2)[n(r)]^2(\sigma_f)E_f[v_c(r)]b_{ij} \quad (25)$$

where:

$E_i(r) = m_i[v_c(r)]^2/2$ = mean collision energy

b_{ij} = 0.25 for differing particles and 0.5 for identical particles

$\sigma_f = \sigma_f[E_i(r)]$ = strongly increasing function of $E_i(r)$

This can be integrated if the variation of both ion density and collision energy is known throughout the potential well.

The integration cannot be performed if convergence is taken as more rapid than inversely proportional to the radial position of the particles. In such a circumstance, the integral goes to infinity at the origin and the calculation has no meaning. Instead, as indicated before, radial flow ion convergence stops as radial momentum is transformed into transverse motion, and the ion flow becomes less strongly focused radially as the center is approached more closely. Transverse ion-ion collisions then result in continuation of radial flow, albeit at a lesser rate of compaction.

Thus, there is some core radius r_c that can characterize the position at which rapid (i.e., geometric) density convergence ceases. Assuming that ion and electron current density conditions are such that there is no significant virtual anode formation at the center, the ion speed is constant in the vicinity of the origin (i.e., for $r_c < r < R$), and the density varies roughly as the inverse square of radial position. This is so because the ions have attained nearly all of their maximum energy by the time they have moved to a position where $\langle r \rangle \leq 7 \times 10^{-2}$. Inside the critical core radius, the ion density can be taken to vary parabolically as an approximation for central density. Dividing the integral into two sections gives the total power,

$$P_f = [4\pi(\sigma_f)n_c^2E_f]b_{ij}\sqrt{\frac{2E_w}{m_i}}r_c^3x\left[1-\frac{r_c}{R}+\frac{71}{105}\right] \quad (26)$$

where m_i is the reduced mass of the system [$m_i = m_1m_2/(m_1 + m_2)$]. The last term in the final brackets is due to integration over the central core volume ($r \leq r_c$), while the first two terms show fusion power generation outside this core region. Comparing these two terms shows that ~40% of the total power comes from the core and 60% from the region adjacent to the core. If the core radius ratio is taken to be small compared to unity, Eq. (26) becomes:

$$P_f = 4.671x10^{-30}[(\sigma_f)n_c^2E_f]r_c^3\sqrt{\frac{E_w}{M_i}}b_{ij} \quad (27)$$

for cgs units, with $M_i = m_i/m_p$. Consider a deuterium-tritium (D-T) system with $M_i = 1.2$, $b_{ij} = 0.25$, a reaction cross section of $\sigma_f = 5$ b (5×10^{-24} cm^2), and a reaction energy of $E_f = 17.6$ MeV, in a well of depth $E_w = 4 \times 10^4$ eV (the peak of the D-T cross-section variation with energy). For these assumptions, the power output is given by:

$$P_f(D-T) = 1.876x10^{-26}(n_c^2)r_c^3(watts) \quad (28)$$

for n_c in ions per cubic centimeter and r_c in centimeters. Suppose that the density is $n_c = 2 \times 10^{17}$/cm^3, and that this is attained at a convergence ratio of $\langle r_c \rangle = (r_c/R) = 10^{-2}$ in a device with radius $R = 100$ cm. The power output from such a system would be P_f(D-T) = 7.50×10^8 W = 750 MW. Of this, ~40% of the power, or 300 MW, would come from a central core of 1-cm radius, a little "star" burning brightly in the center of a 2-m sphere.

As another example, consider p-^{11}B, with a well depth $E_w = 4 \times 10^5$ eV, slightly below the cross-section peak, and a cross section of $\sigma_f = 0.4$ b (0.4×10^{-24} cm^2) in a device with radius $R = 150$ cm, and $\langle r_c \rangle = 7 \times 10^{-3}$. The total fusion power generation is found to be $P_f = 2.684 \times 10^{-27}(n_c^2)(r_c^3) = 3.107 \times 10^{-27}(n_c^2)$ W. If the density is taken to be $n_c = 4 \times 10^{17}$/cm^3, twice that chosen before (and consistent with the larger convergence ratio assumed here), the power generation is P_f(p-^{11}B) = 4.97×10^8 W = 497 MW, comparable to that for the smaller D-T machine example illustrated above.

V.B. Energy Distributions, Multi-Body Collisions, and Upscattering

It is important to create an ion injection environment in which the CM of the system is as close as possible to the CG of the system. With this, almost all collisions are at the system center CG at conditions of equal momentum, and central scattering only redirects the particle momenta to new radius vectors from the well center. Such collisions will not lead to "spreading" of the central core.

Initially, the interaction energy in collisions of equally energetic ions at the center of the well is determined solely by the angle between the radius vectors of motion

of each particle. This leads to a simple expression for the initial particle collision energy distribution:

$$E_c(\theta) = (E_{max})\sin^2\left(\frac{\theta}{2}\right) = \frac{E_{max}}{2}(1-\cos\theta) \quad (29)$$

where:

θ = angle between particle velocity vectors

E_{max} = (E_1 + E_2) = total kinetic energy of both particles in the system.

The fractional number of collisions per unit angular interval is a function of θ:

$$\frac{1}{N(r)}\frac{dn(r)}{d\theta} = [n] = \sin\theta \quad (30)$$

Using these, the initial ion energy and velocity distributions are found to be as shown in Figure 6. Note how different these are from the Maxwellian distribution that characterizes systems in local thermodynamic equilibrium. Because most of the particles in this system are initially centered around the desired collision energy, less power must be put into low-energy particles to sustain an energetic tail, as for Maxwellian equilibrium systems.

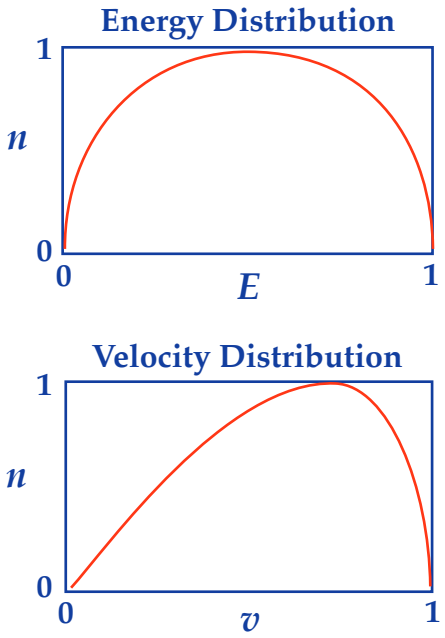

Figure 6 — Energy and velocity distributions for central collisions in radially mono-energetic converging ion flow: CM and CG are coincident in the system

The initial distribution remains radially monoenergetic until a sufficient time has elapsed that two-body collisions have produced sufficient up- and down-scattering to yield a Maxwellian plasma, or until one or more three-body collisions have occurred with each particle. Any such distortion of the initial distribution leads to increased ion losses from the system by increased transverse ion momentum generation in the surface region B field with consequent core divergence and/or by simple escape through the edge of the potential well. The surface magnetic field that holds the electrons in place is too weak to contain energetic ions.

The ions are not long-term residents of the system. They are lost by either energy-broadening up-scattering collision processes (and related orbit expansion and momentum generation) or by fusion reactions. If they are to be consumed by fusion reactions before they are significantly energy broadened, the fusion reaction rate must be made to exceed the collisional up-scattering rate. Conditions necessary for achieving this desired state can be determined by comparing the fusion reaction rate and the two-body collision rate.

Two-body interactions do not broaden the distribution for head-on collisions. However, central (CG frame) two-body collisions at other angles can cause energy up- and down-scattering, because the collisional CM is itself moving relative to the CG frame, and CG frame momentum and energy can be exchanged in such collisions. MacDonald et al.[28] analyzed this process for Coulomb collisions of an initially mono-energetic (but isotropic) plasma and showed that the "Maxwellianization" time t_{mx} is comparable to the energy exchange collision time t_s (Reference 20) in the plasma, with collisional upscattering to high energy E_L above the mean energy E_m proceeding more slowly, as $t_{mL} \approx (t_{mx}/2)(E_L/E_m)^{1.5}$. Thus, the time to reach $E_L \geq 6\,E_m$ is $\geq 7.4\,t_{mx}$, for example. Now, the rate density of two-body collisions in the core (q_2) is just equal to the core density times the two-body collision frequency (f_2). Taking this as the inverse of the energy exchange time in the plasma gives:

$$q2 = \frac{8x0.714\pi n^2 e^4 Z^4 \ln(\Gamma)}{\sqrt{m}(3kT)^{1.5}}$$

$$= 9.0x10^{-8}\left[\frac{n_c Z^4 \ln(\Gamma)}{\sqrt{A}E_c^{1.5}}\right]\left(\frac{collision}{s \bullet cm^3}\right) \quad (31)$$

where:

E_c = core energy (eV)

A = ion mass (amu)

ln(Γ) = Coulomb logarithm

Since the fusion rate density is $q_f = n_{c^2}(\sigma_f v_c)b_{ij}$ the ratio of core two-body to fusion reaction rate density is $q_{2f} = q_2/q_f$ given by:

$$q_{2_f} = 6.5x10^{10}\frac{Z^4 \ln(\Gamma)}{E_c^2 \sigma_f b_{ij}} \quad (32)$$

The fusion cross sections are also strong functions of collision energy. Typically, $\sigma_f = \sigma_{f0}(E_c)^s$, with $s \geq 3$ for many reactions over a limited range of energy below the peak cross section, so that q_{2f} scales with energy at least as rapidly as $(1/E_c^5)$. From this equation and the cross-section energy scaling, it is clear that if $E_c = E_m$ is small, q_{2f} can be large, and vice versa. For example, for Z = 1 and In(Γ) = 10, this shows that $q_{2f} = 4 \times 10^4$ at $E_c = 10^4$ eV with D-T, and $q_{2f} = 120$ at $E_c = 6 \times 10^4$ eV.

With such collisionality, the bulk collisions in the central core tend to distort the core in energy distribution from its initial form. However, it is important to note that the two-body collisions in Equations (31) and (32) do not involve the same ions from one moment to the next, because each ion resides in the core only a small fraction of its transit time across the system. Thus, the rate of collisional energy scattering is much less than would be adduced from the calculation of q_{2f} above.

The time any given ion spends in the core is $\delta t_c = r_o/v_c$, while the time required for a system transit is $\delta t_R = 2\int dr/v(r)$ integrated from 0 to R. For an assumed parabolic potential well shape, the ion speed is given crudely by $v(r) = v_c[1 - \langle r \rangle^2]^{0.5}$. With this, the transit time is estimated as $\delta t_R \approx \pi R/v_c$ so that the fraction of time spent in the core is given by $g_i = r_o/\pi R = \langle r_o \rangle/\pi$. Thus, the number of upscattering two-body collisions per ion per fusion reaction becomes $q_{2f}|_{sc} = q_{2f}\langle r_o \rangle/\pi$, so that the previous examples give only $q_{2f}|_{sc} \approx 130$ for $E_c = 10^4$ eV and $q_{2f}|_{sc} = 0.38$ for $E_c = 6 \times 10^4$ eV. Since Maxwellianization requires at least t_s for ions in the bulk and $(t_s/2)(E_L/E_e)^{1.5}$ for the tail ions, it is clear that full Maxwellianization cannot occur for well depths ≥ 20 keV, and that the high energy tail distribution will never be filled for such mean core energies.

Ions scattered to an energy greater than the well depth are lost from the system but give up their energy to the electric potential field; thus, there will be little effect on system energy balance. The principal result of such upscattering and escape is an increased gas load on the system vacuum pumps, which must be able to handle this gas input to maintain base pressure.

Three-body (and higher order) collisions are not important in the system. This is readily seen by examining the ratio of three-body to two-body collision rate densities q_{32}. The three-body collision rate q_3 is the two-body collision frequency f_2 times the density of extant two-body collision states $\mathcal{Q}_2$. This latter is, itself, equal to the two-body collision rate times the two-body lifetime, which is taken as the time required to traverse a distance equal to the Debye length. Writing these terms using standard formulas from Spitzer,[15] q_{32} is found to be:

$$q_{32} = 2.57x10^{-11}\,\frac{Z^4 \ln(\Gamma)\sqrt{n_i M_i}}{E_c^{1.5}} \qquad (33)$$

It is quite clear that $q_{32} << 1$ for all $E_c > 10$ eV, for any core density of interest (e.g., $q_{32} \approx 10^{-2}$ for $n_i = 10^{18}$/cm³, $E_c = 10$ eV), so that multi-body collisions in the core are not significant to the system. At the system periphery, where E is small, three-body collisions are not important because the ion density is also small.

There remains one other potential source of loss by energy upscattering from two-body collisions at points away from the CG of the device. This is the enhancement of collisional losses of electrons through the surface field and magnetic cusps by randomization (and upscattering) of the electron energy distribution. Such randomization can take place by electron-electron energy exchange or scattering collisions in regions away from the core ($r >> r_o$) over the lifetime of electrons within the system.

This process can be estimated by determining the total path length traversed by an electron during its residence in the system and comparing this with the mean free-path for electron-electron collisions integrated over the state parameters characterizing its path. Introducing the parameter N_j as the number of scattering collisions undergone by an electron during its lifetime in the system and carrying out the algebra leads to a constraint equation relating system design parameters:

$$G_j^2 \leq 5.56x10^6 \left\langle r_0 \right\rangle^3 (E_w R N_j) \ln\left(\frac{1}{\left\langle r_0 \right\rangle}\right) \qquad (34)$$

where the convergence ratio is taken as $\langle r_o \rangle = \langle r_c \rangle$.

As an example, consider a system of radius $R = 100$ cm, $\langle r_o \rangle = 10^{-2}$, and a well depth of $E_w = 10^5$ eV. Keeping the number of electron energy exchange collisions below unity ($N_j < 1$) requires that $G_j < 1.60 \times 10^4$. A larger system with higher convergence but a deeper well may actually be no more limited than this . Consider $E_w = 4 \times 10^5$ eV, $R = 200$ cm, and $\langle r_o \rangle = 10^{-3}$, and take $N_j = 10$. Then the upper limit on current recirculation ratio is $G_j < 4.82 \times 10^5$. If $N_j = 1$ in this latter system, the limit would be $G_j < 1.52 \times 10^5$.

Note that the electron collision probability is much higher at low energy (near the center) than at high energy (near the periphery). Because of this feature, operation at conditions where $N_j > 1$ does not necessarily distort the electron energy distribution significantly, since most of the electron-electron collisions exchange only small amounts of energy relative to the (high) electron injection energy. Thus, allowable maximum values of G_j, as limited by electron scattering collisions, are still sufficiently large for operation of these converging flow systems with large recirculation ratios.

VI. Power Balance, Losses, and System Performance Gain

VI.A. Cusp Electron and Magnet Coil Ohmic Power Losses

In stable steady-state operation, no net losses are associated with the injection of fusion fuels for makeup, as long as the reaction products are charged particles and all fuels are injected to preserve coincident CM/CG collisionality. This is because energy lost by electron ejection is always exactly made up by addition of positive charge ion energy from reaction products escaping from the well. The power input requirement for machine operation is then found to be due solely to the loss mechanisms discussed earlier.

Electron transport losses, core bremsstrahlung, synchrotron radiation, and collisional upscattering particle losses can all be made small by appropriate choice of system operating conditions. Electron cusp losses remain the most significant losses from the region of the confined particles. These are governed by the area of the "holes" in the cusps made by the gyro magnetic motion of the escaping electrons at their surface energy. The cusp loss power is given in terms of the injected surface average electron current density j_o, the electron current recirculation ratio G_j, and other parameters, with $\langle Q \rangle = (j_o G_j/B)$, as:

$$P_b = 35.9\frac{(NE_w^2)(j_0 G_j)}{B^2} = 35.9\frac{NE_w^2}{B}\langle Q\rangle (watts) \tag{35}$$

where the parameters j_o and G_j are related to others by various constraint equations. Using these, a necessary condition for operation is found to be:

$$(BR)^2 > 2.856(NE_w G_j) \tag{36}$$

Consider an octahedral system, $N = 8$, with a well depth of $E_w = 10^5$ eV, and a desired upper limit current gain factor of $G_j = G_{jm} = 5 \times 10^4$. To reach this state, the product of radius and B field strength must be $(BR) > 3.38 \times 10^5$ G•cm. For a system with radius $R = 100$ cm, the field must be $B > 3.38 \times 10^3$, $G = 3.38$ kG. The minimum injection power for this example will be $P_{inj} = 1.257 \times 10^{10} j_o$, for the average injection current density (j_o). For a current input of $j_o = 10^{-3}$ A/cm^2, the power required is 12.57 MW, and the total recirculating electron current in the system is $I_e = (j_o G_j)(4\pi R^2) = 6.28 \times 10^6$ A, or 6.28 MA, for the G_j value assumed above. The corresponding recirculating power is found to be 6.28×10^{11} W or 6.28×10^5 MW, much larger than the fusion power that the system will generate. This very large tangentially isotropic power flow is azimuthally symmetric around the well center; its magnitude ensures that perturbations cannot lead to unstable growth against such a stable symmetric energy flux.

The other principal power loss is that of the magnet coils. This is estimated by determining the resistance of the polyhedral edge coil conductors and their power consumption as a function of their face central B field strength. In the design of such a conductor system, it is desirable to control the free area around the core. This area is that through which fusion product charged particles can pass outward from the system to be converted directly into electrical energy by acting against externally imposed electric fields. It is useful to specify the coil winding in terms of its blockage of this free solid angle. Doing so, the coil power consumption is found as:

$$P_0 = \frac{2\pi\phi_e(RB^2\sqrt{N})}{AR(f_s)(f_i k_b)^2}(watts) \tag{37}$$

where:

f_i = coil fractional solid angle intercept

AR = height/width aspect ratio of the conductor cross section

f_s = conductor fractional solidity (to allow for cooling channels)

ϕ_e = conductor resistivity (Ωcm)

$k_b = (2\pi/10)$ = constant in the defining equation for the magnetic field produced on each face (of equivalent radius r_a) of the polyhedral coil system, $B = k_b(I_j/r_a)$

The total principal losses are then the sum of the above:

$$P_{b0} = \frac{A1}{B^2} + A2(B^2) \tag{38}$$

where:

$$A1 = 35.9(NE_w^2)(j_0 G_j) \tag{38b}$$

for the term due to cusp losses of electrons and:

$$A2 = \frac{2\pi(\phi_e)R\sqrt{N}}{AR(f_s)(f_i k_b)^2} \tag{38c}$$

for the term due to ohmic coil losses.

Since one term varies inversely and the other directly with the square of the B field amplitude, it is evident that an optimum B field value must exist that will minimize the total power loss. This is found by the usual rules of differentiation to be given by $(B_{opt})^4 = (A1/A2)$. The coefficients $A1$ and $A2$ depend on various mechanical design assumptions about the polyhedral coil system. Taking these as $AR = 2$, is $f_s = 0.8$, $f_i = 0.1$, and

ϕ_c = 2 x 10^{-6} Ωcm (as for copper conductor) gives the optimum B field from:

$$B_{opt}^2 = 1.343x10^2 \frac{E_w N^{0.25} \sqrt{j_0 G_j}}{\sqrt{R}} \quad (39)$$

At this field, the minimum power is found to be:

$$P_{b0}(\min) = 2\sqrt{A1xA2} = \sqrt{R_{j0} G_j}(E_w) N^{0.75} K_0 \quad (40)$$

where the factor K_o is a collection of numerical and design specification constants, $K_o = 2\,[(2\pi)(35.9)(\phi_c)/\,[AR(f_s)(f_i k_b)^2]]^{1/2}$. For operation at this optimum (minimum power) condition, the two loss terms are always equal.

Using previously chosen values of design parameters, K_o = 0.535, thus $P_{bo}(min.)$ = 0.535$(Rj_oG_j)^{0.5}$ x $(E_w N^{0.75})$. Now, if the device is taken to operate at E_w = 10^5 eV, with R = 100 cm, electron injection current density and recirculation ratio of j_o = 10^{-3} A/cm2, and G_j = 5 x 10^4, the unavoidable power losses are $P_{bo}(min.)$ = 2.744 x 10^7 W or 27.44 MW for a polyhedron with 14 faces (e.g., a truncated cube). The optimum magnetic field for this set of conditions is $B_{opt.}$ = 4.28 x 10^3 G = 4.28 kG, for which the cusp loss power is $P_b(opt.)$ = 13.72 MW, exactly half of the total power loss. Similarly, the ohmic power loss is found to be 13.72 MW, as well.

Table 2

Reaction Energy and Synthetic Gain at Peak Cross Section for Fusion Fuels

Fusion Fuels	Energy, E_f (MeV)	Peak Cross Section σ(b)	Peak Cross Section (keV)	Synthetic Gain at Peak, $G_o(pk)$
D-T	17.6	5.0	40	440
D-^{3}He	18.3	0.7	160	114
p-^{6}Li	4.0	0.2	1250	3.2
p-^{11}B	8.7	0.8	560	15.5

VI.B. Power Balance and System Gain Considerations

Without losses, conservation of charge in a charged particle fusion system operating with an established potential well would ensure that it continues to operate in a self-sustaining mode, with the well depth maintained by fusion-reaction-generated charged particles. Conversely, if all of the fusion energy were carried by neutral particles (neutrons), the situation would be quite different, as electron injection energy equal to well depth would be required for each ion put into the system. In this hypothetical circumstance, the drive power required would be equal to the gross fusion power generated multiplied by the ratio of well depth E_w to fusion reaction energy E_f, and the maximum system gain would be limited by the inverse of this ratio. Even though this situation is unphysical, it is useful for later analysis to define a synthetic fusion "operating gain" G_o as this ratio, thus $G_o \leq 10^6(E_f/E_w)$.

This synthetic gain parameter illustrates the importance of operation at small well depth, for the energy release per fusion is independent of the well depth, while the synthetic gain is inversely proportional to it. The effect of large well depth may be seen by noting the synthetic gain value that characterizes various fuels at the energy that corresponds to the maximum of their fusion reaction cross section. Such synthetic gain values are given in Table 2, calculated from cross-section data presented in Figure 5.

Power losses due to electron and/or ion escape from a real system are always crudely proportional to the ion or electron energy, hence depend on the depth of the confining potential well. Design for operation at the peak of the fusion reaction cross-section curves will not result in the highest practical gain in systems with finite losses. Better performance (higher system gain) will be achieved by operating at lower well depths, with smaller cross sections, but higher synthetic gain values. Operation at small well depth drives the design of the machine to larger sizes, for both a given power and for the reduction of losses. Cusp losses are a surface-to-volume effect and larger sizes lead to proportionately lesser losses. Thus, the "best" machines are found in that size range where

overall maximum practical system gain is achieved, consistent with requirements limiting overall system size. This can be determined only by analysis of the real gain of the system G_s.

The power available outside the well is always less than that generated from fusion, by the power given up by the ions to the well itself. Thus, the net power available for external use is less than the gross power generated, by the ratio of well depth to reaction energy multiplied by the net ionic charge per fusion $(Z1 + Z2)(E_w/E_f)$. The system gross gain G_{sgr} is defined as the ratio of gross power output generated by fusion reactions to total power input to drive the system, including the power required by ions injected for fuel makeup. The system net gain G_{snL} is defined as the ratio of net fusion power output, available outside of the potential well, to net input power required, taking into account that the fusion product ion drive (as a direct power source to the well) exactly balances the ion input power required for fuel makeup.

First consider the gross gain of a conventional system using normal magnets, operated at optimum B. Total power input must be sufficient to make up for all losses plus ion fuel makeup to support fusion reactions (ion energy return to the well is included here within the gross fusion power source term). In this simplest case, the total power input is limited to three requirements: ion fuel makeup, electron cusp losses, and ohmic power in the magnet coils. The total system gross gain then becomes:

$$G_{sgr} = \frac{G_0}{\left[(Z1+Z2)+G_0\left(\frac{P_{b0}}{P_f}\right)\right]} = \frac{G_0}{[(Z1+Z2)+LTRM]} \quad (41)$$

where $P_b = P_o = P_{bo}/2$ at optimum B operation.

The parameters in the loss term LTRM = $G_o(P_{bo}/P_f)$ are not all independent of each other but are related by various physics requirements. First, the B field must be that found as B_{optL}, which depends on E_w, j_o, G_j, N, and R. In addition, the mean core ion density (average n_c within $r_c = r_o$) is not a free variable, but is fixed by other parameters of the system. This can be scaled by $n_c = n_{io}(R/r_c)^m = G_j n_{eo}/\langle r_c \rangle^m$, where the power law accounts approximately for its relation to a "synthetic" ion density of $n_{io} = G_j n_{eo}$ at the device surface (at $r = R$). A reasonable value of m here is $m = 3$. The maximum value possible for G_j is a function of R, B, N, and E_w. Since $B = B_{optL}$ is itself dependent on E_w, j_o, G_j, N, and R, it is possible to solve for G_j, thus constrained, as a function of only j_o, R, and N. Carrying out the algebra, it is found that $G_j = 2.25 \times 10^3 j_o R^3 / N^{1.5}$. With this the loss term becomes:

$$LTRM = 0.965 x 10^8 \left[\frac{\sqrt{E_w M_i}(N^3)\langle r_0 \rangle^3}{(b_{ij})(\sigma_f)R^7 j_0^3}\right] \quad (42)$$

It is interesting to note that this term and thus the overall system gross gain (of a loss-dominated system) varies as the seventh power of the system radius; small changes in system size will yield very large changes in gain. Gain also varies as the cube of the parameter $(j_o/N\langle r_o \rangle)$ thus, a small number of polyhedral faces is desirable as is a high degree of ion flow convergence (small $\langle r_o \rangle$). Unfortunately, these desires conflict, for fields with small N lead to greater particle-field collisonal dispersion of radial to transverse momentum within the system than large N systems, thus in turn leading to poorer convergence of the ion flow. Optimal conditions can be determined only by detailed analysis.

Finally, while this term varies explicitly directly as the square root of well depth, the fusion reaction cross section changes much more rapidly than this; thus, it is clear that an optimum E_w exists that maximizes real system gain. This is readily seen from the gain equation, written so that all terms other than the E_w terms are suppressed, thus $G_{sgr} = K1/[E_w + K2/E_w^{(s-1.5)}]$, where the fusion reaction cross section has been taken as varying as $(E_w)^s$. The factors not involving E_w have been absorbed into the coefficients $K1$ and $K2$. From this it is found that the optimum well depth is independent of $K1$, as expected, and is given by $E_w(opt) = [K2\ (s - 1.5)]^{[1/(s+1.5)]}$.

For some reactions (e.g., D-T, D^{3}He, p-^{11}B) the exponent s increases as energy decreases below the cross-section peak and becomes as large as 5 or 6 at low energy. Others (e.g., D-D, p-^{6}Li) vary more slowly, but still exhibit increasing $s > 2$ to 3 with decreasing E_w. Because of this, all reactions of interest will yield maximum system gross gain at well depths below the cross-section peak. This drives high-gain systems designs toward low-power-density operation, which then requires large size for large gross power output. This may be acceptable in some applications (e.g., surface ship propulsion, central station power, size-insensitive space power systems, etc.), but in others a requirement of small size and/or mass, with associated high power density, may force the design to systems of less than maximum gain.

As an example of gross gain, take a D-T system ($M_i = 1.2$) with $b_{ij} = 0.25$, $(Z1 + Z2) = 2$, a well depth of $E_w = 2 \times 10^4$ eV, $G_j = 5 \times 10^4$, $N = 14$, electron injection current density of $j_o = 10^{-2}$ A/cm^2, and a radius of $R = 100$ cm. For these conditions, the optimum B field is found to be $B_{optL} = 3.41 \times 10^3$ G. At the assumed well depth, the fusion reaction cross section is $\sigma_f = 2.0$ b. Taking a convergence ratio of

$\langle r_o \rangle = 10^{-2}$, the loss term becomes LTRM = 20.71. In this case the synthetic system gain will be G_o = 880, and the overall system gross gain will be $G_{sgr} = G_o/(2 + \text{LTRM})$ = 38.8. Operation at higher well depth would result in lower G_{sgr}. For this example, power input required is P_{bo} = 50.2 MW and the gross fusion power generation is P_{fus} = 1945 MW.

A more direct connection can be made with system design criteria by recasting the loss term (and gain) equations into yet another form, to display their dependence on system driving power. For the optimal (minimum loss) systems here, the total input power is twice the magnet coil ohmic power or the (equal) electron injection power. This latter is $P_{inj} = P_b = 4\pi R^2(j_o E_{-w})$; thus, the parameters j_o or E_{-w} can be removed from the loss term above. Doing this and taking the fusion cross section as $\sigma_f = \sigma_{f0} j_o E_{-w}^s$ yields:

$$LTRM = 1.915 x 10^{11} \left\{ \frac{\left(N \langle r_0 \rangle / P_{inj} \right)^3 \sqrt{M_i}}{b_{ij} R(\sigma_{f0}) E_w^{(s-3.5)}} \right\} \quad (43)$$

Note that a typical fusion reaction cross-section variation $\sigma_f = (\sigma_{f0} E_{-w}^s$, with s = 3.5, removes all well depth dependence of the loss term. In a loss-dominated system [where LTRM >> $(Z_1 + Z_2)$], the gross gain is then determined as the cube of the parametric term $(P_{inj}/N\langle r_o \rangle$, again depending on the product of the number of cusps (polyhedral faces) and the ion convergence ratio.

In closing, it is important to note that the gain of any real system can be markedly increased if superconductors are used as the magnet coil material, so that direct ohmic power losses are eliminated and only cusp electron losses remain as the principal loss mechanism. The choice of B field is still constrained by power balance arguments, but the magnet-related power required is that to maintain the superconductor below its limiting operating temperature. In this circumstance, power minimization analysis shows that much higher cusp fields may be used, thus allowing reduction of the cusp losses themselves. In the limit of very high fields, core bremsstrahlung dominates losses, and system performance gain is bounded by constraints somewhat different from those outlined above.

Acknowledgments

This work was supported in part by Energy/Matter Conversion Corporation (EMC2) and Pacific-Sierra Research Corporation, and in part under U.S. Defense Nuclear Agency contract DNA-87-C-0052, published by permission.

Revision History

Received October 12, 1989. Accepted for publication on June 26, 1990. Published on March 1991 in Fusion Technology.

Color illustrations added July 2007. Minor updates to illustrations and equations made on December 2008 by Mark Duncan.

References

[1] Robert W. Bussard, "Method and Apparatus for Controlling Charged Particles," U.S. Patent Number 4,826,626 (May 2, 1989).

[2] Robert W. Bussard et al., "Preliminary Research Studies of a New Method for Control of Charged Particle Interactions," Report 1899, Pacific-Sierra Research (Nov. 30, 1988).

[3] Irving Langmuir, "The Effect of Space Charge and Residual Gases on Thermionic Currents in High Vacuum," Physics Review, 2, 450 (1913); Irving Langmuir and Katharine B. Blodgett, "Currents Limited by Space Change Between Coaxial Cylinders," Physics Review, 22, 347 (1923); Irving Langmuir and Katharine B. Blodgett, "Currents Limited by Space Charge Between Concentric Spheres," Physics Review, 24, 49 (1924); and Irving Langmuir, "Thermionic Currents in High Vacuum I. Effect of Space Charge," Physik. Zeitschr., 15, 348 (1914).

[4] J. D. Daugherty and R. H. Levy, "Equilibrium of Electron Clouds in Toroidal Magnetic Fields," Physics Fluids, 10, 155 (1967).

[5] Oleg A. Lavrent'ev, "Electrostatic and Electromagnetic High-Temperature Plasma Traps," translated by Thomas J. Dolan, in Electromagnetic Confinement of Plasmas and the Phenomenology of Relativistic Electron Beams, L. C. Marshall and H. Sahlin, Editors, Annuals New York Academy Science, 251, 152-178 (1975).

[6] T. Consoli, "Review of Electrostatic and Electromagnetic Confinement Experiments Made at the French ABC," in Electromagnetic Confinement of Plasmas and the Phenomenology of Relativistic Electron Beams, L. C. Marshall and H. Sahlin, Editors, Annuals New York Academy Science, 251, 322 (1975).

[7] Philo T. Farnsworth, "Electric Discharge Device for Producing Interactions Between Nuclei," U.S. Patent Number 3,258,402 (June 28, 1966).

[8] Robert L. Hirsch, "Inertial-Electrostatic Confinement of Ionized Fusion Gases," Journal Applied Physics, 38, 4522 (1967).

[9] K. M. Hu and Edward H. Klevans, "On the Theory of Electrostatic Confinement of Plasmas with Ion Injection," Physics Fluids, 17, 227 (1974). 292 DOI: 10.1063/1.1694594

[10] W. M. Black, "Theory of Potential-Well Formation in an Electrostatic Confinement Device," Journal Applied Physics, 45, 2502 (1975).

[11] Christopher W. Barnes, "Computer Simulation of Electrostatic Confinement of Plasmas," in Electromagnetic Confinement of Plasmas and the Phenomenology of Relativistic Electron Beams, Lauriston C. Marshall and Harry Sahlin, Editors, Annuals New York Academy of Sciences, 251, 370 (1975), ISBN 0890720053

[12] William C. Elmore, James L. Tuck, and Kenneth M. Watson, "On the Inertial-Electrostatic Confinement of a Plasma," Physics Fluids, 2, 239 (1959).

[13] Harold P. Furth, "Prevalent Instability of Non-thermal Plasmas," Physics Fluids, 6, 48 (1963).

[14] R. Keller and I. R. Jones, "Confinement d'un plasma par un systeme polyedrique a courant alternatif," Z. Naturfor., 21, 1085 (1966).

[15] Ralph W. Moir and William L. Barr, "'Venetian Blind' Direct Energy Convertor for Fusion Reactors," Nuclear Fusion, 13, 35 (1973).

[16] William L. Barr and Ralph W. Moir, "Test Results on Plasma Direct Convertors," Nuclear Technology Fusion, 3, 98 (1983).

[17] S. Lundgren, Electric Power Research Institute, Private Communication (August 17, 1988).

[18] Samuel Glasstone and Ralph Lovberg, Controlled Thermonuclear Reactions, Chapter 13, Van Nostrand, New York (1960). ISBN 0442027168

[19] David L. Book, "NRL Plasma Formulary," Revised, Naval Research Laboratory (1983).

[20] Lyman Spitzer, Physics of Fully Ionized Gases, Chapter 5, Interscience Publishers, New York (1956). ISBN: 0486449823

[21] R. Jones, "Crossfield Electrostatic Confinement in Cusps," Plasma Physics, 25, 1535 (1983). doi: 10.1088/0032-1028/25/12/417

[22] James Sinnis and George Schmidt, "Experimental Trajectory Analysis of Charged Particles in a Cusped Geometry," Physics Fluids, 6, 841 (1963).

[23] K. N. Leung, N. Hershkowitz, and K. R. MacKenzie, "Plasma Confinement by Localized Cusps," Physics Fluids, 19, 1045 (1976). DOI: 10.1063/1.861575

[24] D. L. Ensley, "Physics Modeling Project," Internal Memorandum, Pacific-Sierra Research (Oct. 1986) and "IACCEU/EACCEL2 User Guide," Internal Memorandum, Pacific-Sierra Research (Apr. 1987); see also J. McDonald and B. Goplen, "ACCEL User's Manual," MRC/WDC-R-180, Pacific-Sierra Research (November 1988).

[25] B. Goplen, "Analytical Theory and Numerical Computational Studies," Attachment B of PSR Report 1899, Pacific-Sierra Research (November 30, 1988).

[26] Yuri L. Klimontovich, "Charged Particle Energy Losses Due to Excitation of Plasma Oscillations," Soviet Physics JETP, 36, 999 (1959).

[27] Robert W. Bussard, "Some Considerations of Dynamic Behavior in the Plasma Thermocouple," Journal Applied Physics, 33, 606 (1962).

[28] William M. MacDonald, Marshall N. Rosenbluth, and David L. Judd, "Fokker-Planck Equations for an Inverse Square Force," Physics Review, 107, 1 (1957); DOI: 10.1103/PhysRev.107.1; see also W. M. MacDonald, M. N. Rosenbluth, and W. Chuck, "Relaxation of a System of Particles with Coulomb Interactions," Physics Review, 107, 350 (1957).